Journal of Power Sources 240 (2013) 598–605

Contents lists available at SciVerse ScienceDirect

Journal of Power Sources

journal homepage: www.elsevier.com/locate/jpowsour

Sulfur/activated-conductive carbon black composites as cathode materials for lithium/sulfur battery

G.C. Li, J.J. Hu, G.R. Li, S.H. Ye, X.P. Gao*

Institute of New Energy Material Chemistry, Tianjin Key Laboratory of Metal and Molecule Based Material Chemistry, Nankai University, Tianjin 300071, China

HIGHLIGHTS

- The commercial CCB is activated with KOH as matrix to load sulfur as cathode for Li/S battery.
- After activation treatment, the surface area and pore volume of the CCB are increased.
- The S/A-CCB composite with 64 wt% S presents the optimized electrochemical performance.

ARTICLE INFO

Article history:
Received 14 December 2012
Received in revised form
1 February 2013
Accepted 24 February 2013
Available online 13 May 2013

Keywords:
Lithium–sulfur battery
Cathode
Sulfur–carbon composite
Conductive carbon black
Activation treatment

ABSTRACT

The commercial conductive carbon black (CCB) with large surface area and good electrical conductivity after activation treatment is employed as conductive matrix to support sulfur for the cathode of lithium/sulfur battery. The S/activated CCB composites with 64 and 73 wt% sulfur are prepared by a simple heat treatment method. The microstructure and morphology of the as-prepared S/activated CCB composites are characterized by thermogravimetry (TG), X-ray diffraction (XRD), scanning electron microscopy (SEM), and transmission electron microscopy (TEM). It is demonstrated that sulfur can be loaded into the pores of the host activated CCB matrix in highly dispersed state, when sulfur loading is limited to 64 wt%. While the loaded sulfur increases to 73 wt%, some crystalline sulfur nanoparticles of less than 2 nm can be observed near the pores of the host activated CCB matrix. As expected, the S/activated CCB composite with 64 wt % sulfur presents the optimized electrochemical performance, including the utilization of active sulfur, discharge capacity and cycle stability. Apparently, in order to improve the electrochemical performance of the S/activated CCB composite, the activation treatment of the commercial CCB is essential for increasing the sulfur loading.

1. Introduction

The lithium/sulfur battery system, based on the light-weight elements and multi-electron reactions, has a large theoretical energy density of 2600 W h kg^{-1} [1–6], which is almost one order of magnitude higher than those of currently commercialized transition metal oxide and phosphate cathodes, such as $LiCoO_2$, $LiMn_2O_4$, and $LiFePO_4$ [2]. In addition, element sulfur as cathode material has the advantages of low cost, environmental benign, and abundance in nature [5]. Therefore, the lithium/sulfur battery is regarded as one of the most promising candidates for the next generation of high energy density rechargeable battery. Although the lithium/sulfur battery has been investigated for more than two decades [3,6], the practical development of the lithium/sulfur battery is slow because of some serious problems, including the low utilization of sulfur active material and its poor cycle stability, due to the highly insulating nature of sulfur (5×10^{-30} S cm^{-1} at 25 °C), and the high solubility of lithium polysulfides as intermediate products generated during the electrochemical reduction reaction process [3–7].

In recent years, several technological strategies have been made to improve the electrochemical performance of the sulfur cathode for developing high energy lithium/sulfur battery with the particular attention on the utilization and cycle stability of the active sulfur cathode. The fundamental researches are generally divided to two directions, i.e. (1), optimizing the organic electrolyte or inorganic additives [7–13]; and the fabricating sulfur-based composites, including sulfur/conductive polymer composites [14–20], sulfur/carbon composites [21–37], and polymer/sulfur/carbon multicomposites [38–43]. In these studies, various carbon

* Corresponding author.
E-mail address: xpgao@nankai.edu.cn (X.P. Gao).

0378-7753/$ – see front matter © 2013 Elsevier B.V. All rights reserved.
http://dx.doi.org/10.1016/j.jpowsour.2013.02.095

materials are shown to be more effective for improving the cycle stability, active sulfur utilization and high-rate capability of the sulfur cathode, due to their good electrical conductivity, large pore volume, and strong mesoporous/microporous adsorption capability of carbon matrix. Indeed, the hierarchical porous structure of carbon materials with large surface area and good conductivity is beneficial for loading active sulfur and thus effectively improving the electrochemical performance of the sulfur cathode in different electrolyte system. In addition, the large sulfur loading (at least over 60 wt %) on carbon materials is also indispensable for increasing the capacity of sulfur cathode and energy density of lithium/sulfur battery. However, only a limited quantity of the qualified carbon materials can be synthesized, and such problem limits the subsequent mass production of sulfur/carbon composites and the further commercialization of lithium/sulfur battery. Therefore, seeking the stable, abundant, and applicable carbon raw materials with manipulative pore structure and large surface area is essential for the mass production of sulfur/carbon composites, as well as Li/S battery in present day.

In this work, we introduce the commercial conductive carbon black (CCB) with large specific surface area and pore volume, which can be used as the matrix for electrode-active materials [42,44]. To further increase the specific surface area and pore volume based on the requirement of the large sulfur loading, chemical activation with KOH at high temperature under Ar atmosphere is employed. Subsequently, the sulfur is loaded on the host activated CCB (denoted hereafter as A-CCB) matrix by heating the mixture of the sublimed sulfur and A-CCB to produce S/A-CCB composites with different sulfur loadings. As anticipated, the as-prepared S/A-CCB composite with 64 wt % S presents the optimized electrochemical performance.

2. Experimental section

2.1. Activation of the conductive carbon black (CCB)

The commercial conductive carbon black (Black Pearls 2000, Cabot Corporation) was activated with KOH. Firstly, the powder-shaped carbon was obtained by ball-milling CCB (BP 2000) particles in a planetary type ball mill (300 rpm, 12 h). The obtained carbon powders (1.5 g) were mixed with KOH aqueous solution (6.0 g KOH dissolved in 50 mL distilled water), treated ultrasonically for 1 h, and heated to 80 °C with continuous stirring. After water was completely evaporated, the mixture of CCB and KOH was transferred into a nickel crucible. The crucible was heated to 800 °C at a heating rate of 10 °C min^{-1} in a tube furnace under Ar atmosphere. The temperature was kept at 800 °C for 2 h, and then cooled to room temperature. The residue in the crucible was diluted with distilled water, washed and filtered for more than five times to neutral, and then centrifuged with absolute ethyl alcohol. Finally, the activated CCB was dried in a vacuum oven at 60 °C for 12 h.

2.2. Preparation and characterization of sulfur/carbon composites

The as-prepared A-CCB was mixed with sublimed sulfur (chemical grade) in the weight ratio of 1:3 and 1:5, respectively. The mixture of the sublimed sulfur and A-CCB was heated to 150 °C with a heating rate of 5 °C min^{-1} and kept for 8 h in a sealed stainless steel vessel with an interior volume of ca. 200 mL, filled with argon gas. At this temperature, the melt sulfur with the lowest viscosity can easily diffuse into the meso/micropores of the prepared A-CCB. The temperature was then increased to 300 °C and kept for 3 h to vaporize the sulfur covered on the surface of the prepared A-CCB. After cooling down to room temperature, the two composites with different sulfur contents were obtained. The sulfur content in the composites was confirmed using a thermogravimetric analyzer (Mettler Toledo, TGA/DSC1) under Ar atmosphere with a flow rate of 50 mL min^{-1} at a heating rate of 10 °C min^{-1} from 30 to 600 °C. The microstructure and morphology of the A-CCB and the as-prepared S/A-CCB composites were detected using X-ray diffraction (XRD, Rigaku MiniFlex II), Brunauer–Emmett–Teller analysis (BET, JW-BK 122W and Micromeritics ASAP2020), scanning electron microscopy (SEM, Hitachi S-4800), and transmission electron microscopy (TEM, FEI Tecnai F20). Scanning transmission electron microscopy (STEM) was performed in Tecnai F20 using a high-angle annular dark field (HAADF) detector, coupled with an energy dispersive X-ray spectrometer (EDX). The sulfur and carbon element mapping was conducted by the local chemical analysis, using STEM-EDX with HAADF detector.

2.3. Electrochemical measurements

In order to prepare the working electrode, the composite was mixed with acetylene black and polytetrafluorethylene (PTFE) in a weight ratio of 70:20:10 with ethanol as dispersant. The paste was compressed into a thin piece with a roller. The obtained piece was then cut into a disk film of 8 mm in diameter, which was dried in a vacuum oven at 50 °C for 12 h before assembling the testing cells. The half-cells were assembled in a glove box filled with argon. Lithium metal was used as the counter electrode as well as the reference electrode and a microporous polypropylene film (Celgard 2300) was used as a separator. The electrolyte was prepared in a glove box filled with highly purified argon by dissolving 0.2 M anhydrous $LiNO_3$ and 1 M $LiN(CF_3SO_2)_2$ (LiTFSI) in a mixed solvents of 1,3-dioxolane (DOL) and tetra-ethylene glycol dimethyl ether (TEGDME) by volume ratio of 1:1. All of the electrolyte salts, solvent and additive were purchased from the J&K Scientific Ltd. (Beijing) and used without further treatment. Galvanostatic charge/discharge cycling tests were carried out to evaluate the electrochemical capacity and cycle stability of the electrodes on the basis of the active sulfur at ambient temperature using the LAND-CT2001A instrument (Wuhan Jinnuo, China). The cut-off potentials for the charge and discharge processes were set to be 3.0 and 1.0 V (vs Li/Li^+), respectively. The cyclic voltammetry (CV) measurement was conducted with the CHI 600A electrochemical workstation (Shanghai ChenHua, China) at a scan rate of 0.1 mV s^{-1}.

3. Results and discussion

The sulfur content of the as-prepared S/A-CCB composites is measured by thermogravimetric analysis (TG) under Ar

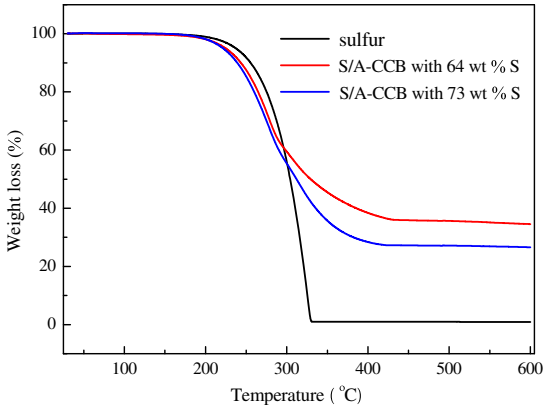

Fig. 1. TG curves of the as-prepared S/A-CCB composites recorded under Ar atmosphere with a heating rate of 10 °C min^{-1}.

atmosphere as shown in Fig. 1. The weight loss of the composites can be observed with increasing temperature from about 180 °C, and the curves become stable when the composites are heated over 400 °C due to evaporation of sulfur from the mesopores or micropores of the host A-CCB. The sulfur content of the A-CCB composites are 64 and 73 wt%, respectively, calculated from the TG curves. It is also noted that the highest desorption temperature is much higher than that of pure sulfur, indicating the strong adsorption of meso/micropores of the host A-CCB matrix and/or the existence of the weak interaction between carbon and sulfur, especially for the composite with 64 wt% S.

The specific surface areas of the commercial CCB and the as-prepared A-CCB are 1024.4 and 1401.2 $m^2\ g^{-1}$, respectively (Table 1). In particular, the pore volume of the commercial CCB is increased from 1.21 $cm^3\ g^{-1}$ to 1.64 $cm^3\ g^{-1}$, due to local broadening or local burn-off in KOH activation treatment [45,46]. The enlargement of the specific surface area and pore volume is beneficial for the sulfur loading on the carbon matrix. After loading sulfur on the host A-CCB matrix, the specific surface areas dramatically reduce to 69.5 and 67.9 $m^2\ g^{-1}$ for the S/A-CCB composites with 64 and 73 wt% S, respectively. Simultaneously, the corresponding pore volumes sharply decrease to 0.10 and 0.08 $cm^3\ g^{-1}$, respectively. Such a dramatic decrease in the surface area and pore volume means that sulfur has been encapsulated into the pores of the host A-CCB matrix.

XRD patterns of the CCB, as-prepared A-CCB and S/A-CCB composites are presented in Fig. 2. Two broad diffraction peaks located at around 25 and 43°can be seen for both CCB and A-CCB, corresponding to (002) and (101) diffractions of graphitic carbon, respectively. No peaks at 53 and 78°corresponding to the (004) and (110) diffractions can be observed, suggesting that both CCB and A-CCB have a turbostratic structure with a large curvature of the graphite layer, similar to the amorphous characteristic of two samples [24,25]. Clearly, there are no characteristic peaks of the crystalline sulfur in the S/A-CCB composite with 64 wt% S. It is believed that sulfur melts and diffuses into the pores of the host A-CCB matrix at 150 °C due to the lowest viscosity of sulfur and the strong adsorbability of the host A-CCB matrix. When the temperature reaches 300 °C, sulfur that exists at the external surface could be sublimed and re-adsorbed into the pores of the host A-CCB matrix. Therefore, the elemental sulfur in the S/A-CCB composite exists in highly dispersed state, resulting in the amorphous composite [24,25,34,35]. On the contrary, when the sulfur content in the S/A-CCB composite further increases to 73 wt%, the weak characteristic peaks of the crystalline sulfur can be detected due to a crystallization of extra sulfur enclosed in the host A-CCB matrix, indicating that sulfur exists in a mixed state of both crystalline and amorphous structures in the S/A-CCB composite with 73 wt% S.

SEM images of the CCB, as-prepared A-CCB and S/A-CCB composites are shown in Fig. 3. Apparently, the commercial CCB appears as loose particles aggregated of small carbon spheres with a size of about 100 nm, which is very similar to the conductive carbon black (Ketjenblack EC600JD) used as conductive carbon matrix, as reported previously [42,44]. After being activated, the spherical

Table 1
Specific surface area and pore volume of the CCB, as-prepared A-CCB and S/A-CCB composites.

Samples	S_{BET} ($m^2\ g^{-1}$)	V_t ($cm^3\ g^{-1}$)
CCB	1024.4	1.21
A-CCB	1401.2	1.64
S/A-CCB with 64% S	69.5	0.10
S/A-CCB with 73% S	67.9	0.08

S_{BET} is the specific surface area, and V_t is the total pore volume.

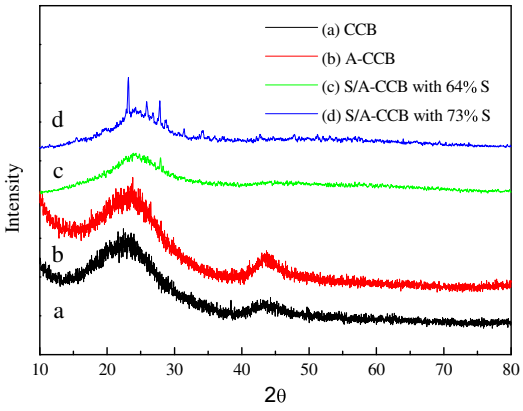

Fig. 2. XRD patterns of the CCB, as-prepared A-CCB and S/A-CCB composites.

morphology of the as-prepared A-CCB can still be retained, indicating that only the microstructure (surface area and pore volume) is varied without altering the spherical morphology and size of the commercial CCB during the KOH activation. In the S/A-CCB composite with 64 wt % S, there is no apparent difference in morphology and size for both the as-prepared S/A-CCB and the A-CCB composites. Thus, elemental sulfur completely diffuses, absorbs, and disperses in the pores of the host A-CCB matrix by a capillary force during the heating process. However, when the sulfur loading increases to 73 wt%, the inner pores of the host A-CCB matrix are fully filled with sulfur, and the extra sulfur is crystallized in the host A-CCB matrix, leading to more serious agglomeration of the S/A-CCB composite with 73 wt% S, as compared to the composite with 64 wt% S.

Fig. 4 shows TEM images of the as-prepared A-CCB and S/A-CCB composites. It is found that the nano-particles of A-CCB interlace to form a chain-like structure, similar to acetylene black [26], which can ensure good conductivity of the carbon matrix. Moreover, the partially graphitized structure with some micropores/mesopores is shown in nanoparticles of the A-CCB, in consistent with above XRD analysis. After loading 64 wt% sulfur, the carbon matrix with partially graphitized structure is clearly shown, almost the same as that of the A-CCB matrix. Only a small amount of the small crystalline sulfur nanoparticles (dark dots that are less than 2 nm) can be observed near the pores of the host A-CCB matrix, indicating that the pore volume of the host A-CCB matrix is large enough to accommodate highly dispersed sulfur. Although the pores of the host A-CCB matrix are filled with sulfur, the sulfur in the highly dispersed state is almost indistinguishable from TEM image due to the low mass contrast between carbon and sulfur. However, when the sulfur loading increases to 73 wt%, some small crystalline sulfur nanoparticles (dark dots that are less than 2 nm) appear clearly based on the mass-thickness contrast, due to the crystallization of extra sulfur near the pores of the host A-CCB matrix. Of course, the surface of the host A-CCB matrix is still clean without sulfur deposition. It means that the pores of the host A-CCB matrix is preferably filled with sulfur in the highly dispersed state, and the extra sulfur is compelled to aggregate and crystallize as nanoparticles near the pores of the host A-CCB matrix.

The elemental sulfur distribution is further confirmed by the local chemical analysis performed by STEM-EDX (Fig. 5). Clearly, carbon and sulfur elements are detected across a selected area of the S/A-CCB samples, confirming the existence of sulfur in the S/A-CCB composites. In particular, the elemental sulfur shows homogeneous distribution for the composite with 64 wt% S. On the other hand, the partial enrichment of sulfur in the composite with 73 wt% S still presents due to the partial aggregation and

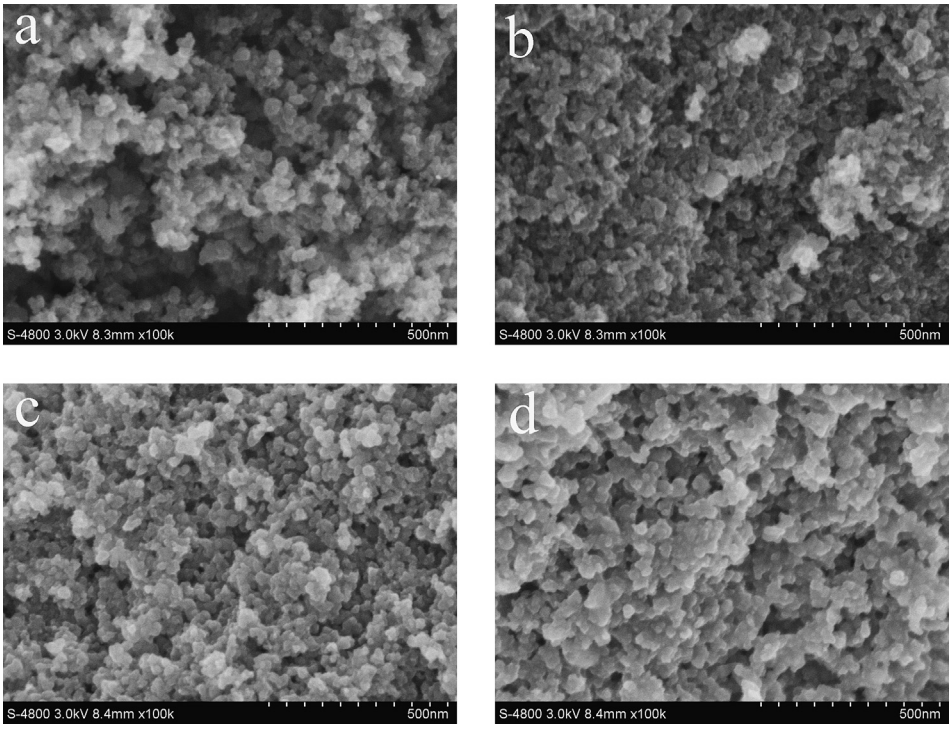

Fig. 3. SEM images of the CCB (a), as-prepared A-CCB (b) and S/A-CCB composites with 64 wt% S (c) and 73 wt% S (d).

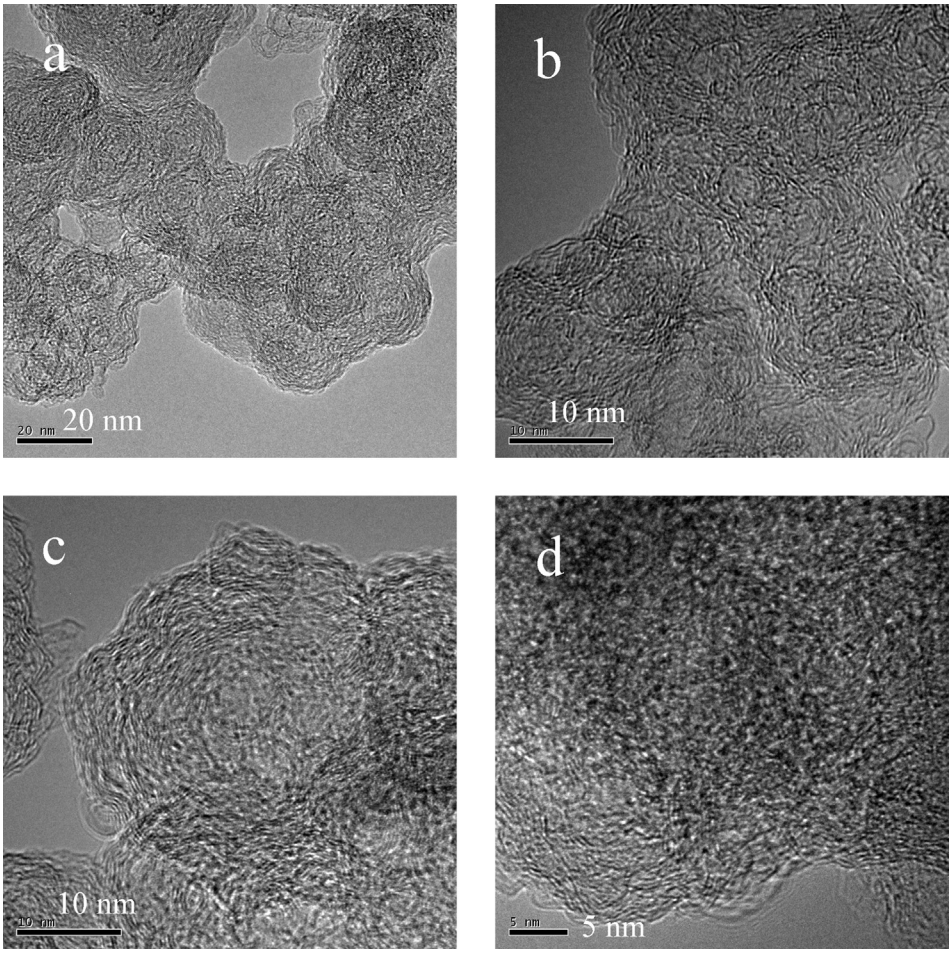

Fig. 4. TEM images of the as-prepared A-CCB (a and b) and S/A-CCB composites with 64 wt% S (c) and 73 wt% S (d).

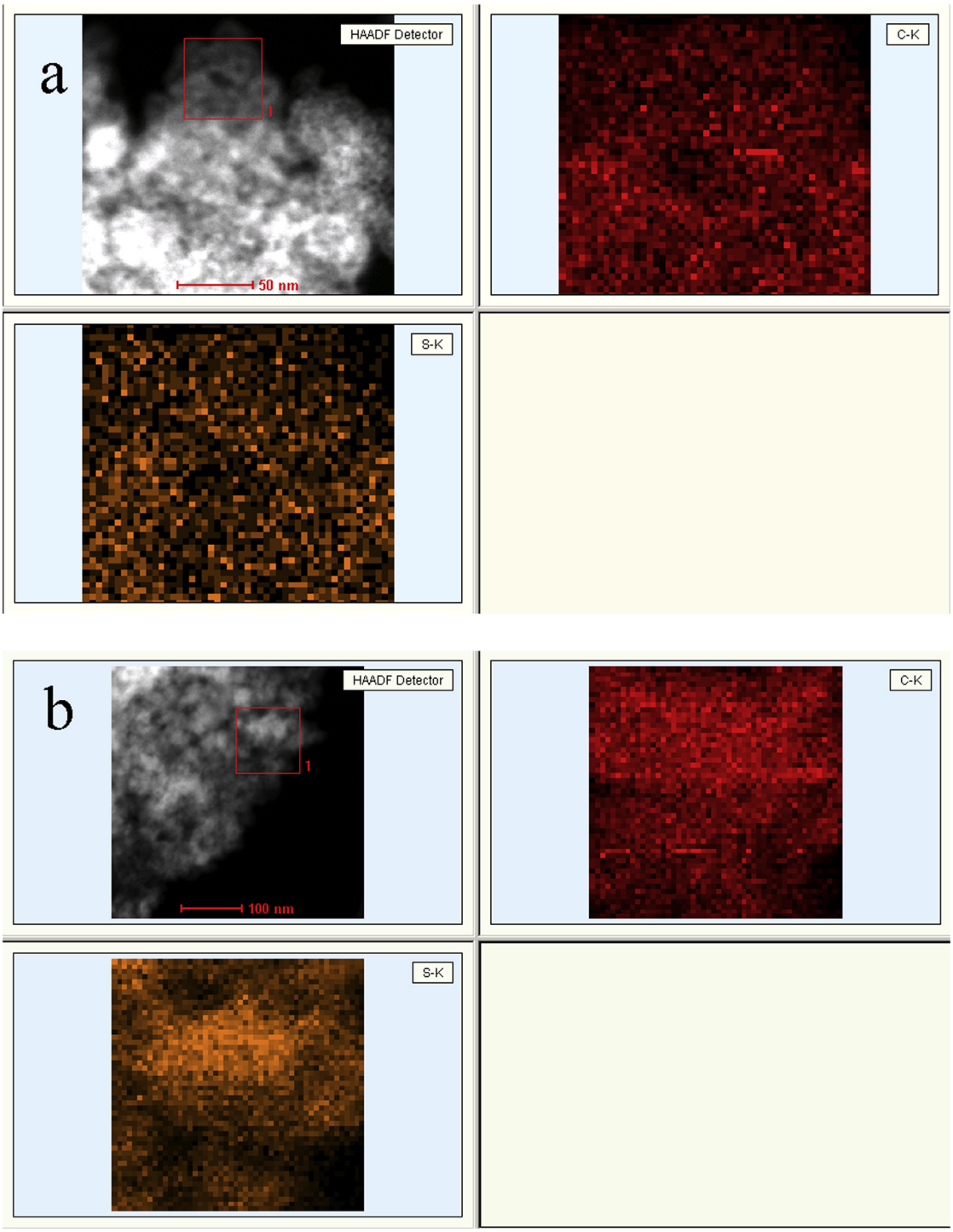

Fig. 5. HAADF-STEM image and corresponding mapping of carbon and sulfur elements across a selected area (red square in STEM) of the as-prepared S/A-CCB composites with 64 wt% S (a) and 73 wt% S (b). (For interpretation of the references to color in this figure legend, the reader is referred to the web version of this article.)

crystallization of extra sulfur near the pores of the host A-CCB matrix, in consistent with above TEM observation and XRD analyses.

Cyclic voltammograms of two electrodes are shown in Fig. 6. In the initial cathodic process of the composite with 64 wt% S, two broad reduction peaks appear at 2.25 and 1.80 V (vs Li/Li^+), respectively, due to the two-step reduction of sulfur with metallic lithium [21,30,31]. In addition, a small tailing peak at 1.1 V (vs Li/Li^+) appears, confirming the existence of the weak interaction between carbon and sulfur in the A-CCB composite. In the following cycles, the cathodic peak potentials move up to about 2.30 and 1.85 V (vs Li/Li^+), which is ascribed to the polarization of the electrode in the first cycle. In particular, the cathodic and anodic peak areas remain almost unchanged, confirming a relatively good reversibility and stability after the initial electrochemical process. For the composite with 73 wt% S, both the cathodic and anodic peak currents quickly reduce, implying a poor electrochemical stability of the S/A-CCB composite during cycling.

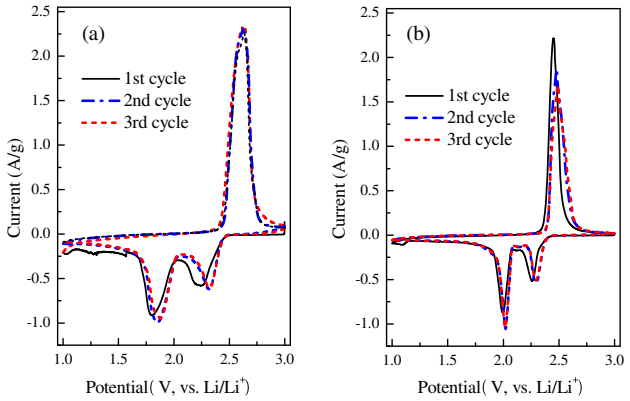

Fig. 6. Cyclic voltammograms of the as-prepared S/A-CCB composites with 64 wt% S (a) and 73 wt% S (b) at a scan rate of 0.1 mV s^{-1}.

The initial three charge and discharge curves of the as-prepared composites are shown in Fig. 7, measured at the current density of 160 mA g^{-1}. Two typical discharge potential plateaus at about 2.08 and 2.33 V (vs Li/Li^+) with a hysteretic slope can be easily observed in the initial cycle for the S/A-CCB composite with 64 wt% S, which can be assigned to the reduction from sulfur to high-order lithium polysulfides, with possibly further reduction to low-order lithium polysulfides and even to lithium sulfides in the end [21,25,41]. The presence of the hysteretic slope in the discharge processes is attributed to the existence of the weak interaction between carbon and sulfur in the A-CCB composite. Only one potential plateau is presented in the charge process at about 2.38 V (vs Li/Li^+), analogous to CV features in Fig. 6, which is attributed to the interlaced conversion from lithium sulfides to low-order lithium polysulfides, high-order lithium polysulfides and sulfur. Correspondingly, the initial discharge capacity of the composite with 64 wt% S is 956.7 mA h $g^{-1}_{(sulfur)}$, larger than that (698 mAh $g^{-1}_{(sulfur)}$) of the composite with 73 wt% S, implying good utilization of the active sulfur in the composite with 64 wt% S. In addition, the coulombic efficiency is about 95% for the composite with 64 wt% S in the subsequent cycles. As shown in Fig. 8, there is an activation process with increasing the discharge capacity during cycling, indicating that the electrochemical activity of the composite is gradually improved. In the 2nd cycle, the maximum discharge capacity of the composite with 64 wt% S is 1383.6 mA h $g^{-1}_{(sulfur)}$ after the initial activation. After then, the discharge capacity monotonously decreases due to the solubility of lithium polysulfides and gradual aggregation of insulated Li_2S on the cathode surface during the electrochemical reduction process in organic electrolyte [3,7,24]. After 100 cycles, the discharge capacity of 531.9 mA h $g^{-1}_{(sulfur)}$ is retained for the composite with 64 wt% S. However, the S/A-CCB composite with 73 wt% S can endure only 50 cycles, when the discharge capacity decreases to 479.6 mA h $g^{-1}_{(sulfur)}$. The electrochemical performance of the S/A-CCB composite with 64 wt% S is much better as compared to the S/A-CCB composite with 73 wt% S, including discharge capacity, coulombic efficiency and cycle stability. Hereafter, the S/A-CCB composite with 64 wt% S is chosen to be further investigated the high rate performance.

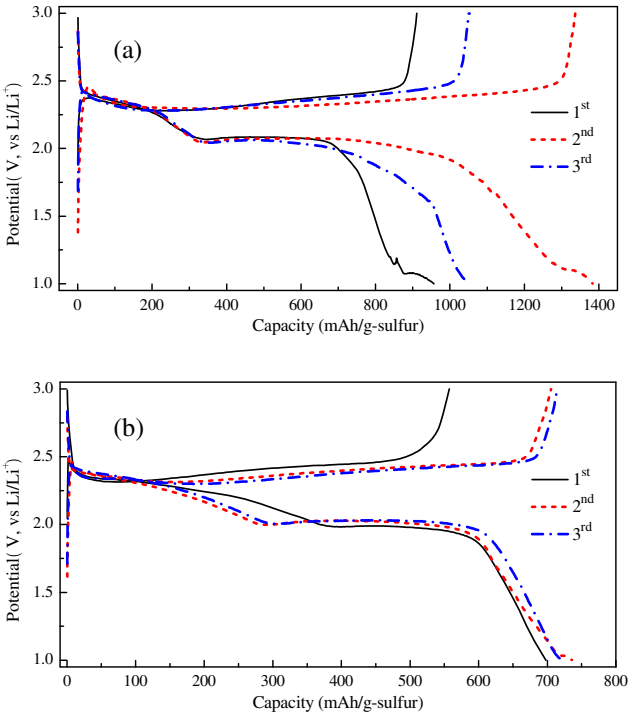

Fig. 7. The initial three charge–discharge curves of the as-prepared S/A-CCB composites with 64 wt% S (a) and 73 wt% S (b) at the current density of 160 mA g^{-1}.

The high-rate discharge capability and cycle performance of the S/A-CCB composite with 64 wt% S are measured at various current densities in Fig. 9. As anticipated, the composite presents an excellent high-rate capability. The initial discharge capacity is 987 mA h $g^{-1}_{(sulfur)}$, and the maximum discharge capacity is 1175.4 mA h $g^{-1}_{(sulfur)}$ after activation at the low current density of 160 mA g^{-1}. The discharge capacity of 668.1 mA h $g^{-1}_{(sulfur)}$ and the maximum discharge capacity of 778.7 mA h $g^{-1}_{(sulfur)}$ are obtained at the current density of 400 mA g^{-1}, indicating the activation process still persist with increasing the current density. It is noted that the electrolyte with TEGDME solvent used here is more viscous than the conventional electrolyte with 1,2-dimethoxyethane (DME) solvent [47]. Therefore, the electrochemical activity of the S/C composite would be gradually improved due to the slow penetration and transport of electrolyte and lithium ions through the pores of the host A-CCB matrix [42,47], leading to increased utilization with cycling, especially at the high rates. Subsequently, the discharge capacity became relatively stable at various current densities. In particular, the discharge capacity of 398 mA h $g^{-1}_{(sulfur)}$ can still be obtained at the high current density of 1600 mA g^{-1}. When cycling at the current density of 800 mA g^{-1}, the discharge capacity of the S/A-CCB composite with 64 wt% S increases from 552.7 mA h $g^{-1}_{(sulfur)}$ in the initial cycle to 771.8 mA h $g^{-1}_{(sulfur)}$ in 13th cycle. Similarly, the electrochemical activation, though still exists, becomes slow in the high-rate charge/discharge process due to the low utilization of the active sulfur in the S/C composite. After 50 cycles, the discharge capacity still retains at 600 mA h $g^{-1}_{(sulfur)}$, showing good capacity retention.

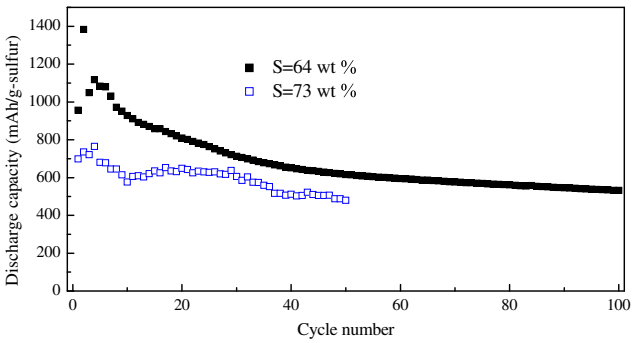

Fig. 8. Cycle performances of the as-prepared S/A-CCB composites with 64 wt% S and 73 wt% S at the current density of 160 mA g^{-1}.

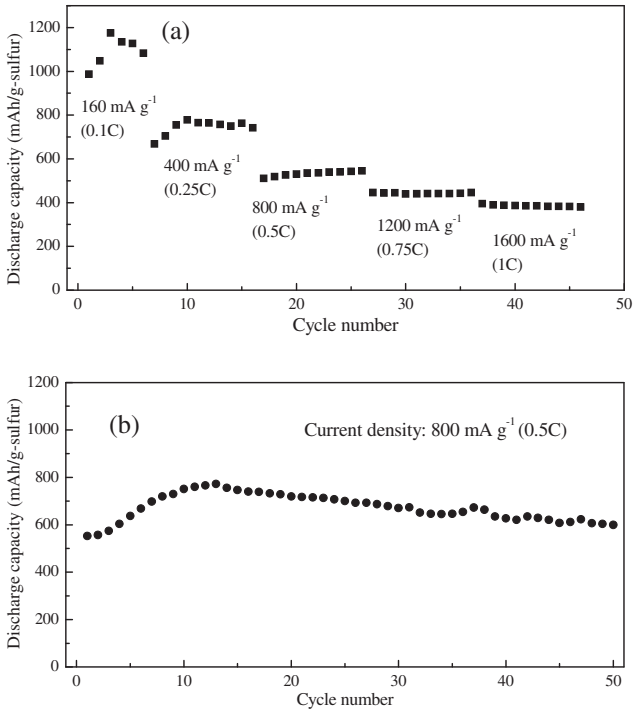

Fig. 9. (a) Rate capabilities of the as-prepared S/A-CCB composite with 64 wt% S and 73 wt% S. (b) The cycle performance of the as-prepared S/A-CCB composites with 64 wt % S at the current density of 800 mA g^{-1}.

It should be noted here that the use of the low-cost and commercial CCB as conductive matrix is significant for the mass production of the S/C composite as well as Li/S battery. Meanwhile, the large sulfur loading on conductive matrix is important for the high energy density of lithium/sulfur battery. Indeed, the specific surface area and pore volume of the commercial CCB can be increased to a certain extent after KOH activation treatment, which is beneficial for increasing the sulfur loading. In addition, the dispersed and crystalline state of the loaded sulfur on the host A-CCB matrix is crucial for the utilization, discharge capacity, and cycle stability of the cathode-active materials. When the sulfur loading is 73 wt%, the utilization of the active sulfur is low and the sulfur inside pores could be blocked to the electrochemical reaction due to the appearance of the some small crystalline nanoparticles near pores or cover pore mouths of the host A-CCB matrix. Meanwhile, the composite with 64 wt% S, with open pore mouths and highly dispersed state of sulfur on the host A-CCB matrix, presents high utilization of the active sulfur. Therefore, the pores of the host A-CCB matrix should be kept open for the indispensable penetration and transportation of electrolyte and soluble lithium polysulfides in the ether-based electrolyte during the electrochemical reaction process to realize the high utilization of the active sulfur, especially for the large sulfur loading. Undoubtedly, further adjustment and optimization of the surface area and pore microstructure of the conductive carbon matrix are needed for the improvement of the electrochemical performance of the S/C composites with the large sulfur loading.

4. Conclusion

The commercial CCB is activated with KOH here as conductive matrix to load sulfur as cathode for lithium/sulfur battery. After activation treatment, the specific surface area and pore volume of the commercial CCB increase a certain extent without altering the spherical morphology, which is composed of chain-like interlaced nanoparticles. Such structural characteristics are beneficial for loading sulfur as well as ensuring good conductivity of the carbon matrix. Subsequently, two sulfur/A-CCB composites with different sulfur loadings are prepared by a simple heat treatment method. It is demonstrated that the dispersed and crystalline state of the loaded sulfur on the host A-CCB matrix are crucial for the utilization, discharge capacity, and cycle stability of the cathode-active materials. In particular, when the sulfur loading is 64 wt%, the composite with open pore mouths and highly dispersed state of sulfur inside the pores on the host A-CCB presents the optimized electrochemical performance. Therefore, the pores of the host A-CCB matrix should be kept open during the electrochemical reaction process for improving the electrochemical performance of the S/C composites, especially for the large sulfur loading.

Acknowledgments

Financial Supports from the 973 Program (2009CB220100), 863 Program (2011AA11A256), and NSFC (51072083) of China are gratefully acknowledged.

References

[1] P.G. Bruce, S.A. Freunberger, L.J. Hardwick, J.M. Tarascon, Nat. Mater. 11 (2012) 19.
[2] X.P. Gao, H.X. Yang, Energy Environ. Sci. 3 (2010) 174.
[3] R.D. Rauh, K.M. Abraham, G.F. Pearson, J.K. Surprenant, S.B. Brummer, J. Electrochem. Soc. 126 (1979) 523.
[4] P. Novak, K. Muller, K.S.V. Santhanam, O. Haas, Chem. Rev. 97 (1997) 207.
[5] D. Marmorstein, T.H. Yu, K.A. Striebel, F.R. McLarnon, J. Hou, E.J. Cairns, J. Power Sources 89 (2000) 219.
[6] H. Yamin, E. Peled, J. Power Sources 9 (1983) 281.
[7] J. Shim, K.A. Striebel, E.J. Cairns, J. Electrochem. Soc. 149 (2002) A1321.
[8] L.X. Yuan, J.K. Feng, X.P. Ai, Y.L. Cao, S.L. Chen, H.X. Yang, Electrochem. Commun. 8 (2006) 610.
[9] D. Aurbach, E. Pollak, R. Elazari, G. Salitra, C.S. Kelley, J. Affinito, J. Electrochem. Soc. 15 (2009) 694.
[10] B.A. Trofimov, M.V. Markova, L.V. Morozova, G.F. Prozorova, S.A. Korzhova, M.D. Cho, V.V. Annenkov, A.I. Mikhaleva, Electrochim. Acta 56 (2011) 2458.
[11] X. Liang, Z.Y. Wen, Y. Liu, M.F. Wu, J. Jin, H. Zhang, X.W. Wu, J. Power Sources 196 (2011) 9839.
[12] S.S. Zhang, J. Electrochem. Soc. 159 (2012) A920.
[13] S.S. Zhang, Electrochim. Acta 70 (2012) 344.
[14] J.L. Wang, J. Yang, J.Y. Xie, N.X. Xu, Adv. Mater. 14 (2002) 963.
[15] L. Wang, X.M. He, J.J. Li, M. Chen, J. Gao, C.Y. Jiang, Electrochim. Acta 72 (2012) 114.
[16] L.L. Qiu, S.C. Zhang, L. Zhang, M.M. Sun, W.K. Wang, Electrochim. Acta 55 (2010) 4632.
[17] Y.Z. Fu, Y.S. Su, A. Manthiram, J. Electrochem. Soc. 159 (2012) A1420.
[18] X. Liang, Y. Liu, Z.Y. Wen, L.Z. Huang, X.Y. Wang, H. Zhang, J. Power Sources 196 (2011) 6951.
[19] F. Wu, J.Z. Chen, R.J. Chen, S.X. Wu, L. Li, S. Chen, T. Zhao, J. Phys. Chem. C 115 (2011) 6057.
[20] L.F. Xiao, Y.L. Cao, J. Xiao, B. Schwenzer, M.H. Engelhard, L.V. Saraf, Z.M. Nie, G.J. Exarhos, J. Liu, Adv. Mater. 24, 1176.
[21] J.L. Wang, J. Yang, J.Y. Xie, N.X. Xu, Y. Li, Electrochem. Commun. 4 (2002) 499.
[22] J. Wang, S.Y. Chew, Z.W. Zhao, S. Ashraf, D. Wexler, J. Chen, S.H. Ng, S.L. Chou, H.K. Liu, Carbon 46 (2008) 229.
[23] X.L. Ji, K.T. Lee, L.F. Nazar, Nat. Mater. 8 (2009) 500.
[24] B. Zhang, X. Qin, G.R. Li, X.P. Gao, Energy Environ. Sci. 3 (2010) 1531.
[25] C. Lai, X.P. Gao, B. Zhang, T.Y. Yan, Z. Zhou, J. Phys. Chem. C 113 (2009) 4712.
[26] B. Zhang, C. Lai, Z. Zhou, X.P. Gao, Electrochim. Acta 54 (2009) 3708.
[27] H.L. Wang, Y. Yang, Y.Y. Liang, J.T. Robinson, Y.G. Li, A. Jackson, Y. Cui, H.J. Dai, Nano Lett. 11 (2011) 2644.
[28] Y.L. Cao, X.L. Li, I.A. Aksay, J. Lemmon, Z.M. Nie, Z.G. Yang, J. Liu, Phys. Chem. Chem. Phys. 13 (2011) 7660.
[29] Z.K. Wei, J.J. Chen, L.L. Qin, A.W. Nemage, M.S. Zheng, Q.F. Dong, J. Electrochem. Soc. 159 (2012) A1236.
[30] N. Jayaprakash, J. Shen, S.S. Moganty, A. Corona, L.A. Archer, Angew. Chem. Int. Ed. 50 (2011) 5904.
[31] S.C. Wei, H. Zhang, Y.Q. Huang, W.K. Wang, Y.Z. Xia, Z.B. Yu, Energy Environ. Sci. 4 (2011) 736.
[32] G. He, X.L. Ji, L. Nazar, Energy Environ. Sci. 4 (2011) 2878.
[33] L.W. Ji, M.M. Rao, S. Aloni, L. Wang, E.J. Cairns, Y.G. Zhang, Energy Environ. Sci. 4 (2011) 5053.
[34] Y.S. Su, Y.Z. Fu, A. Manthiram, Phys. Chem. Chem. Phys. 14 (2012) 14495.
[35] Y.S. Su, A. Manthiram, Electrochim. Acta 77 (2012) 272.

[36] G.M. Zhou, D.W. Wang, F. Li, P.X. Hou, L.C. Yin, C. Liu, G.Q. Lu, I.R. Gentle, H.M. Cheng, Energy Environ. Sci. 5 (2012) 8901.
[37] S. Xin, L. Gu, N.H. Zhao, Y.X. Yin, L.J. Zhou, Y.G. Guo, L.J. Wan, J. Am. Chem. Soc. 134 (2012) 18510.
[38] M.M. Rao, X.Y. Song, H.G. Liao, E.J. Cairns, Electrochim. Acta 65 (2012) 228.
[39] S.R. Chen, Y.P. Zhai, G.L. Xu, Y.X. Jiang, D.Y. Zhao, J.T. Li, L. Huang, S.G. Sun, Electrochim. Acta 56 (2011) 9549.
[40] Y. Yang, G.H. Yu, J.J. Cha, H. Wu, M. Vosgueritchian, Y. Yao, Z.N. Bao, Y. Cui, ACS Nano 5 (2011) 9187.
[41] F. Wu, J.Z. Chen, L. Li, T. Zhao, R.J. Chen, J. Phys. Chem. C 115 (2011) 24411.
[42] G.C. Li, G.R. Li, S.H. Ye, X.P. Gao, Adv. Energy Mater. 2 (2012) 1238.
[43] L.C. Yin, J.L. Wang, F.J. Lin, J. Yang, Y.N. Nuli, Energy Environ. Sci. 5 (2012) 6966.
[44] Y.L. Wang, Q.L. Sun, Q.Q. Zhao, J.S. Cao, S.H. Ye, Energy Environ. Sci. 4 (2011) 3947.
[45] J.C. Wang, S. Kaskel, J. Mater. Chem. 22 (2012) 23710.
[46] S.H. Yoon, S. Lim, Y. Song, Y. Ota, W.M. Qiao, A. Tanaka, I. Mochida, Carbon 42 (2004) 1727.
[47] J.W. Choi, J.K. Kim, G. Cheruvally, J.H. Ahn, H.J. Ahn, K.W. Kim, Electrochim. Acta 52 (2007) 2075.